Separation Science and Technology
Publication details, including instructions for authors and subscription information:
http://www.informaworld.com/smpp/title~content=t713708471

Equilibrium Distribution Coefficients of Some Nitrate Impurities in Sodium Nitrate from Zone Refining

T. Utsunomiya[a]; Y. Hoshino[a]
[a] RESEARCH LABORATORY OF ENGINEERING MATERIALS, TOKYO INSTITUTE OF TECHNOLOGY, YOKOHAMA, JAPAN

To cite this Article Utsunomiya, T. and Hoshino, Y.(1984) 'Equilibrium Distribution Coefficients of Some Nitrate Impurities in Sodium Nitrate from Zone Refining', Separation Science and Technology, 19: 6, 403 — 416
To link to this Article: DOI: 10.1080/01496398408060660
URL: http://dx.doi.org/10.1080/01496398408060660

SEPARATION SCIENCE AND TECHNOLOGY, 19(6 & 7), pp. 403-416, 1984

Equilibrium Distribution Coefficients of Some Nitrate Impurities in Sodium Nitrate from Zone Refining

T. UTSUNOMIYA and Y. HOSHINO

RESEARCH LABORATORY OF ENGINEERING MATERIALS
TOKYO INSTITUTE OF TECHNOLOGY
4259 NAGATSUTA, MIDORI-KU, YOKOHAMA, JAPAN

Abstract

The equilibrium distribution coefficients of 10 impurities (Li, K, Rb, Cs, Ag, Tl, Mg, Ca, Sr, and Ba) in sodium nitrate were determined from the measured values of the effective distribution coefficients obtained by zone refining. The equilibrium distribution coefficients obtained are as follows: $LiNO_3$, 9.2×10^{-2}; KNO_3, 3.0×10^{-1}; $RbNO_3$, 2.2×10^{-2}; $CsNO_3$, 1.3×10^{-3}; $AgNO_3$, 7.8×10^{-1}; $TlNO_3$, 5.2×10^{-1}; $Mg(NO_3)_2$, 7.4×10^{-2}; $Ca(NO_3)_2$, 1.5×10^{-2}; $Sr(NO_3)_2$, 3.0×10^{-2}; and $Ba(NO_3)_2$, 2.1×10^{-2}. These values are in favorable agreement with those estimated from the phase diagrams and/or those calculated from the heat of solid solution.

INTRODUCTION

There are some situations where a sudden demand for increased purity of a chemical occurs because of the development of a new industrial application for a chemical for which purity has not been a serious concern. Sodium nitrate, which is now one of the major raw materials of multicomponent glasses for optical communications, is a good example (*1*). In the case where this compound is used as the sodium source for optical glass fiber, some special characteristics are required for the material to have ultrahigh purity because 3*d* transition metal nitrate impurities affect the absorption loss of light (*2*).

Besides recrystallization, solvent extraction, etc. for the purification of this compound, zone refining has also been used (*3*). The behavior of 3*d* transition metal nitrate impurities has been reported elsewhere (*4*). In the present paper, as a part of studies on a high level of purification of inorganic salts utilizing the molten state, the equilibrium distribution coefficients (k_0) of impurities other than 3d transition metal nitrates have been determined from

 0149-6395/84/1906-0403$3.50/0

measured values of the effective distribution coefficients (k) and compared with those estimated from phase diagrams and/or the calculated heat of solid solution.

Although it is of a great importance to know the distribution coefficient of the impurity in the host crystal for the purification of materials, our literature survey has revealed that almost no systematic work has been done on the distribution behavior of impurities in sodium nitrate. Ten nitrate impurities (Li, K, Rb, Cs, Ag, Tl, Mg, Ca, Sr, and Ba) have been investigated and are discussed. The reason why these impurities were chosen is that (a) commercially available sodium nitrate is often contaminated with these impurities, (b) these impurities are stable in molten sodium nitrate, (c) quantitative determination of these impurities can be performed with relative ease, (d) a number of phase diagrams of them have been published, and (e) these impurities are adequate as model samples for our purification experiments.

DETERMINATION OF EQUILIBRIUM DISTRIBUTION COEFFICIENT

The following three methods are generally used to obtain the equilibrium distribution coefficient (*3*). The first method is to utilize a phase diagram. If an accurate phase diagram quite near the end composition is known, the equilibrium distribution coefficient can be obtained by the ratio of liquid and solid solubility. In conventional phase diagrams, however, which are described by a linear composition scale, the equilibrium distribution coefficient cannot be estimated for binary eutectic systems. The equilibrium distribution coefficient in such a case ranges from 10^{-1} to 10^{-5} (*5*). The second method is to obtain the equilibrium distribution coefficient directly from the thermodynamic calculations based on dilute solution theory. This method can only be applied to a few systems because it is rather difficult to estimate the heat of solid solution of a system. The third method is to obtain k_0 by measuring the effective distribution coefficient (k). In the present paper, k_0 was obtained by the third method. According to Burton et al. (*6*), if the zone travel rate is constant and the diffusion of impurities in the solid can be neglected, the relation between k_0 and k can be written as

$$k_0/k = k_0 + (1 - k_0) \exp[-f\delta/D] \qquad (1)$$

where k_0 and k are the equilibrium and effective distribution coefficients, respectively, f is the zone travel rate, δ is the diffusion layer thickness, and D is the diffusion coefficient of the solute. Equation (2) can be obtained by replacing Eq. (1) with

$$\ln (1/k - 1) = \ln (1/k_0 - 1) - f\delta/D \qquad \text{for } k < 1 \qquad (2)$$

Therefore the equilibrium distribution coefficient can be obtained by measuring the effective distribution coefficient in crystals zone-refined at different zone travel rates under identical conditions and plotting $\ln (1/k - 1)$ against the zone travel rate.

EXPERIMENTAL

Zone Refiner

The zone refiner used in this work was especially assembled for the purification of substances with melting point below 600°C. The apparatus consists of (a) four heaters, (b) a heater driving unit, (c) a temperature control unit, (d) an automatic recycle unit of heaters and (3) an atmosphere substitution unit. The heaters are made of Nicrome or Kanthal wire of 0.5 mm diameter. One of the features of this apparatus is employing air-blasting nozzles to keep the zone length constant. This results in a large temperature gradient at the solid–liquid interface. The heater moves forward and backward by a stepping motor (Copal SP-4-415) at rates of 30 to 100 and 1200 mm/h, respectively. Details of the apparatus have been reported elsewhere (*7, 8*).

Preparation of Samples for the Determination of *k*

The chemicals used in this investigation were all commercially available reagents and used without further purification. Impurities were added to sodium nitrate by dry blending, and the mixture was melted in an electric furnace at 350°C. The pulverized mixtures were stored in clean glass tubes of 12 mm i.d. and about 500 mm in length after keeping them at 200°C for 24 h under vacuum.

Determination of *k*

The zone-refining operations were conducted under various zone travel rates. Several samples were obtained for each system. The determination of impurities was carried out in the following manner. Approximately 1 g of sample was taken from the purified specimen and dissolved in deionized

water. The concentrations of Li, K, Rb, Cs, and Tl were determined by flame photometry and those of Ag, Mg, and Ca were determined by atomic absorption spectrometry.

RESULTS AND DISCUSSION

Some typical values of ln $(1/k - 1)$ against various zone travel rates (f) are plotted in Fig. 1, although the measured values of k were slightly scattered. The other data are listed in Tables 1a--1j to avoid the complexity of Fig. 1. The equations under each table were obtained by linear regression. Most of the determination factor (r^2) of the linear regression equation ranged from 0.89 to 0.99. The equilibrium distribution coefficients calculated from Eq. (2) are listed in Table 2. As is obvious from Table 2, in the case where monovalent cations were substituted for the sodium ion, the solid solubility decreases with an increase of the difference between the cationic radii. This trend can be easily analogized from Hume-Rothery's rule. The equilibrium distribution coefficients were almost constant when divalent cations were substituted. This might be due to the vacancy formation which accompanied

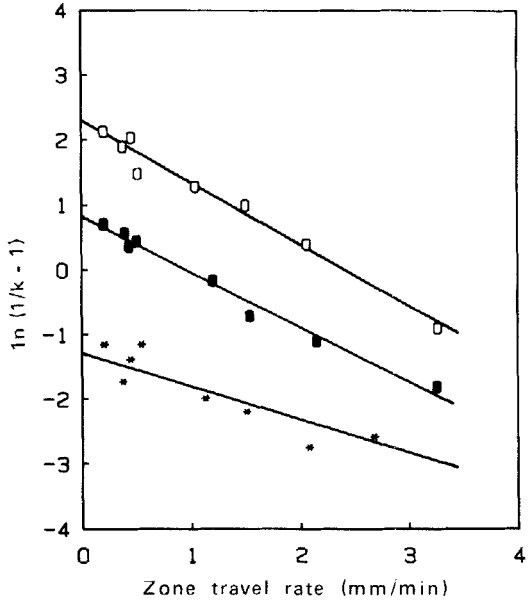

FIG. 1. Dependence of ln $(1/k - 1)$ on zone travel rate for typical nitrate impurities: (○) $LiNO_3$, (●) KNO_3, (*) $AgNO_3$.

TABLE 1a
Determination of Equilibrium Distribution Coefficients for the System $NaNO_3$–$LiNO_3$

No.	f (mm/min)	k	$\ln(1/k - 1)$
1	0.20	0.11	2.13
2	0.37	0.13	1.90
3	0.45	0.12	2.04
4	0.51	0.18	1.49
5	1.04	0.22	1.29
6	1.50	0.27	1.00
7	2.06	0.40	0.40
8	3.26	0.71	−0.90

$\ln(1/k - 1) = 2.29 - 0.95 \times f$
$r^2 = 0.98$
$k_0 = 9.2 \times 10^{-2}$

TABLE 1b
Determination of Equilibrium Distribution Coefficients for the System $NaNO_3$–KNO_3

No.	f (mm/min)	k	$\ln(1/k - 1)$
1	0.20	0.33	0.71
2	0.39	0.36	0.58
3	0.43	0.41	0.36
4	0.50	0.39	0.45
5	1.20	0.54	−0.16
6	1.54	0.67	−0.71
7	2.15	0.75	−1.10
8	3.25	0.86	−1.82

$\ln(1/k - 1) = 0.82 - 0.85 \times f$
$r^2 = 0.98$
$k_0 = 3.0 \times 10^{-1}$

TABLE 1c
Determination of Equilibrium Distribution Coefficients for the System $NaNO_3$–$RbNO_3$

No.	f (mm/min)	k	$\ln(1/k-1)$
1	0.22	0.047	3.01
2	0.43	0.062	2.72
3	0.47	0.065	2.67
4	0.50	0.069	2.60
5	1.24	0.12	1.98
6	1.71	0.15	1.74
7	2.27	0.62	−0.50
8	3.37	0.96	−3.20

$\ln(1/k-1) = 3.76 - 1.87 \times f$
$r^2 = 0.93$
$k_0 = 2.2 \times 10^{-2}$

TABLE 1d
Determination of Equilibrium Distribution Coefficients for the System $NaNO_3$–$CsNO_3$

No.	f (mm/min)	k	$\ln(1/k-1)$
1	0.19	0.001	6.91
2	0.39	0.009	4.70
3	0.49	0.001	6.91
4	0.56	0.003	5.81
5	0.71	0.006	5.11
6	1.22	0.079	2.46
7	1.71	0.38	0.49
8	2.05	0.48	0.08
9	3.41	0.85	−1.74

$\ln(1/k-1) = 6.86 - 2.89 \times f$
$r^2 = 0.89$
$k_0 = 1.3 \times 10^{-3}$

TABLE 1e
Determination of Equilibrium Distribution Coefficients for the System $NaNO_3$–$AgNO_3$

No.	f (mm/min)	k	$\ln (1/k - 1)$
1	0.20	0.76	−1.15
2	0.37	0.85	−1.74
3	0.44	0.80	−1.39
4	0.54	0.76	−1.15
5	1.13	0.88	−1.99
6	1.51	0.90	−2.20
7	2.08	0.94	−2.75
8	2.68	0.93	−2.59
9	5.38	0.98	−3.89

$\ln (1/k - 1) = -1.27 - 0.52 \times f$
$r^2 = 0.92$
$k_0 = 7.8 \times 10^{-1}$

TABLE 1f
Determination of Equilibrium Distribution Coefficients for the System $NaNO_3$–$TlNO_3$

No.	f (mm/min)	k	$\ln (1/k - 1)$
1	0.21	0.55	−0.19
2	0.40	0.54	−0.18
3	0.46	0.55	−0.20
4	0.56	0.59	−0.35
5	1.23	0.58	−0.32
6	1.60	0.57	−0.29
7	2.08	0.70	−0.85

$\ln (1/k - 1) = -0.09 - 0.27 \times f$
$r^2 = 0.64$
$k_0 = 5.2 \times 10^{-1}$

TABLE 1g
Determination of Equilibrium Distribution Coefficients for the System $NaNO_3$–$Mg(NO_3)_2$

No.	f (mm/min)	k	$\ln(1/k-1)$
1	0.21	0.17	1.59
2	0.41	0.12	1.99
3	0.45	0.14	1.82
4	0.57	0.16	1.66
5	1.23	0.70	−0.85
6	2.17	0.87	−1.90

$\ln(1/k-1) = 2.53 - 2.15 \times f$
$r^2 = 0.92$
$k_0 = 7.4 \times 10^{-2}$

TABLE 1h
Determination of Equilibrium Distribution Coefficients for the System $NaNO_3$–$Ca(NO_3)_2$

No.	f (mm/min)	k	$\ln(1/k-1)$
1	0.21	0.024	3.71
2	0.38	0.051	2.92
3	0.46	0.064	2.68
4	0.56	0.057	2.81
5	2.10	0.84	−1.64

$\ln(1/k-1) = 4.14 - 2.75 \times f$
$r^2 = 0.99$
$k_0 = 1.5 \times 10^{-2}$

TABLE 1i
Determination of Equilibrium Distribution Coefficients for the System $NaNO_3$–$Sr(NO_3)_2$

No	f (mm/min)	k	$\ln(1/k-1)$
1	0.21	0.050	2.94
2	0.40	0.040	3.18
3	0.45	0.080	2.44
4	0.55	0.060	2.75
5	1.13	0.17	1.59
6	1.60	0.33	0.71
7	2.04	0.57	−0.28
8	2.96	0.78	−1.27

$\ln(1/k-1) = 3.46 - 1.67 \times f$
$r^2 = 0.98$
$k_0 = 3.0 \times 10^{-2}$

TABLE 1j
Determination of Equilibrium Distribution Coefficients for the System $NaNO_3$–$Ba(NO_3)_2$

No.	f (mm/min)	k	$\ln(1/k-1)$
1	0.20	0.054	2.86
2	0.41	0.057	2.81
3	0.42	0.065	2.67
4	0.55	0.057	2.81
5	1.26	0.20	1.37
6	1.62	0.71	−0.88
7	2.00	0.79	−1.34
8	2.80	0.96	−3.29

$\ln(1/k-1) = 3.82 - 2.54 \times f$
$r^2 = 0.97$
$k_0 = 2.1 \times 10^{-2}$

TABLE 2
Equilibrium Distribution Coefficients and Heat of Solid Solution of Impurities in Sodium Nitrate

Impurity	k_0			ΔH^s (kcal/mol)	
	This work	*a*	*b*	*c*	*d*
$LiNO_3$	9.2×10^{-2}	<0.1	1.7×10^{-1}	2.73	1.2
KNO_3	3.0×10^{-1}	0.30	3.2×10^{-1}	1.33	1.4
$RbNO_3$	2.2×10^{-2}	<0.1	6.8×10^{-2}	4.30	3.1
$CsNO_3$	1.3×10^{-3}	<0.1	1.7×10^{-2}	7.93	5.0
$AgNO_3$	7.8×10^{-1}	0.78	1.0	0.27	0
$TlNO_3$	5.2×10^{-1}	0.59	—	0.73	—
$Mg(NO_3)_2$	7.4×10^{-2}	<0.1	—	—	5.0
$Ca(NO_3)_2$	1.5×10^{-2}	<0.1	—	6.95	0
$Sr(NO_3)_2$	3.0×10^{-2}	<0.1	—	—	—
$Ba(NO_3)_2$	2.1×10^{-2}	<0.1	—	—	—

[a] k_0 estimated from phase diagrams.
[b] calculated values from Eqs. (3) and (4).
[c] calculated values from Eq. (3).
[d] calculated values from Eq. (4).

the substitution. This fact also indicates that the vacancy formation contributes more to the equilibrium distribution coefficients than the size difference.

A number of binary phase diagrams in which sodium nitrate is one of the end components have been published (*9*). The equilibrium distribution coefficients can be obtained from the ratio of impurity concentration of the solidus to that of the liquidus in systems which form a solid solution over a wide composition range. The $NaNO_3$–KNO_3 phase diagram constructed from microthermal analysis agrees well with that reported by Janz. The equilibrium distribution coefficient of KNO_3 estimated from the phase diagram is 0.30 (*10*). The equilibrium distribution coefficients of $AgNO_3$ and $TlNO_3$ from the phase diagrams which were reported by Hissink and Palkin were 0.78 and 0.57, respectively (*11, 12*). These values also agreed well with those obtained in this study. However, it is impossible to estimate the equilibrium distribution coefficient of binary eutectic systems such as $NaNO_3$–$LiNO_3$, –$RbNO_3$, and –$CsNO_3$. The equilibrium distribution coefficients of these impurities are supposed to be below 0.1 as described in a previous paper (*5*). The equilibrium distribution coefficients estimated from the phase diagrams are also listed in Table 2.

Swalin derived a general equation from thermodynamical considerations for the distribution coefficient of an impurity (*13*). According to the author, the equilibrium distribution coefficient can be obtained by setting the chemical potential of the impurity in both the solid and liquid phase equal to each other in the equilibrium state. In this manner the following equation is derived:

$$\ln k_0 = (\Delta H^f - \Delta H^s)/RT - \Delta S^f/R \qquad (3)$$

where ΔH^f and ΔS^f are the heat of fusion and the entropy of fusion of the impurity, respectively, and ΔH^s is the heat of solid solution of the impurity. The other symbols have their usual meanings. Thermond and Struthers revised the above equation to a more precise form (*14*). Weiser, however, pointed out that with corrected terms, the change in vibrational entropy and the activity coefficient could be neglected in the case of the dilute solution model (*15*). Since the heat and entropy of fusion can be obtained from literature data (*16*), the calculation of a theoretical equilibrium distribution coefficient depends on an estimation of the heat of solid solution. Weiser found very satisfactory agreement between theoretically calculated distribution coefficients and experimental values for such semiconductors as germanium and silicon (*15*). On the other hand, Douglas, Neogy, and Allakhverdov derived a theoretical equation to evaluate the heat of solid solution of impurities in alkali halides (*17–19*). Their results also agreed

quite well with the experimental values. For alkali nitrates systems, however, it is rather difficult to estimate the heat of solid solution because various parameters, such as lattice energies, Debye temperatures, and Grüneisen constants, have not been known compared to those of akali halides. Figure 2 shows the dependence of ln k_0 on cation size difference. A good relationship exists between these two parameters in the case of alkali ion impurities except for Li. The cause of the low values of the equilibrium distribution coefficient of Li might be due to the different strain energy contribution of the lattice when the substituted cation is larger or smaller than for the sodium ion. As pointed out by Weiser, the heat of solid solution is the sum of the strain energy and the difference of bonding energy associated with the formation of a substitutional solid solution of foreign atoms. If an impure substance forms a solid solution with $NaNO_3$ over a wide composition range, the strain energy would be negligibly small and the difference of bonding energy would contribute predominantly to the heat of solid solution. According to Eq. (3), ΔH^s has a linear relationship to ln k_0, and the latter is also related to Δr^2 as shown in Fig. 2. Ursov (*20*) proposed the following heat of solid solution equations:

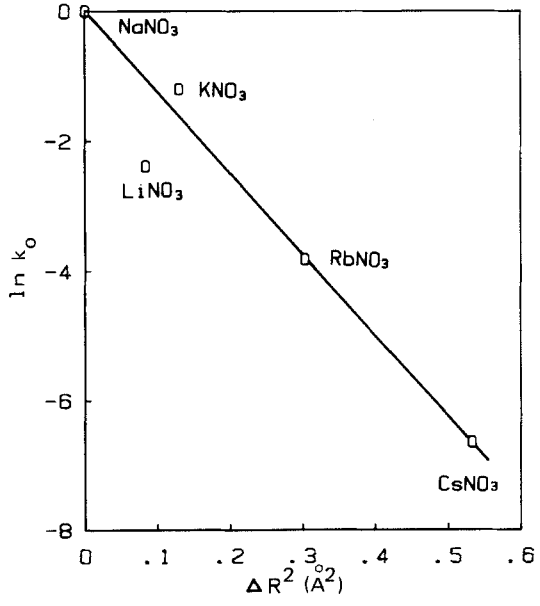

FIG. 2. Dependence of ln k_0 on the difference of cation radius.

$$\Delta H_{\text{mix}} = 65x_1(1 - x_1)z^2n(\Delta R/R)^2$$
$$\Delta H^s = H_{\text{mix}}/x_1(1 - x_1) \tag{4}$$

where ΔH_{mix} is the heat of mixing, z is the charge of the ion substituted, and n is its coordination number. The heats of solid solution calculated from Eqs. (4) are listed in Table 2. Because the equilibrium distribution coefficients estimated from the phase diagrams agreed quite well with those obtained in this study, ΔH^s was calculated from Eq. (3) and is also listed in Table 2. Agreement of these values is satisfactory as first-order approximations.

If the heat of solid solution is accurately evaluated, the liquidus and the solidus of impurities at very low concentrations can be calculated from

$$\ln(1 - x^l) = \frac{\Delta H_A^f}{R}\left(\frac{1}{T_m} - \frac{1}{T}\right) \tag{5.1}$$

$$\ln\frac{x^s}{x^l} = \frac{\Delta H_B^f - \Delta H^s}{RT} - \frac{\Delta S^f}{R} \tag{5.2}$$

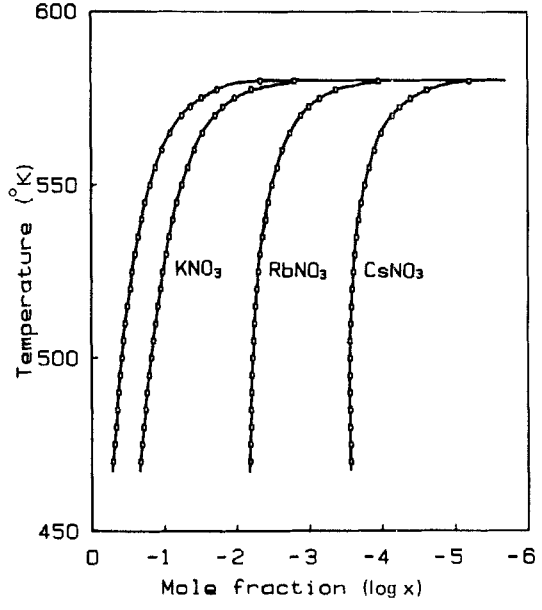

FIG. 3. $NaNO_3$–MNO_3 (M = K, Rb, Cs) phase diagrams for $NaNO_3$-rich portion. The left curve indicates the liquidus of $NaNO_3$, and the others indicate the solidus curves for each impurity.

TABLE 3
Heat of Solid Solution of Some Impurities in Sodium Nitrate

Impurity	k_0	ΔH^f (kcal/mol)	ΔS^f (cal·deg^{-1}·mol^{-1})	ΔH^s (kcal/mol)
$LiNO_3$	9.2×10^{-2}	5.96[c]	11.66[b]	2.73
KNO_3	3.0×10^{-1}	2.30[a]	3.786[a]	1.33
$RbNO_3$	2.2×10^{-2}	1.11[c]	1.91[b]	4.30
$CsNO_3$	1.3×10^{-3}	3.21[c]	4.96[b]	7.93
$AgNO_3$	7.8×10^{-1}	2.80[a]	5.797[a]	0.27
$TlNO_3$	5.2×10^{-1}	2.26[c]	4.71[c]	0.73

[a] I. Barin and O. Knacke, *Thermochemical Properties of Inorganic Substances*, Springer-Verlag, Berlin, 1973.
[b] G. J. Janz, F. J. Kelly, and J. L. Perano, *J. Chem. Eng. Data*, *9*(1) 133 (1964).
[c] O. J. Kleppa and F. G. McCarty, *ibid.*, *8*(3), 331 (1963).

where x^l and x^s are mole fraction of an impurity equilibrated with the liquid and solid phases, respectively, ΔH_A^f is the heat of fusion of the host crystal, T_m is the melting point of the host crystal, ΔH_B^f is the heat of fusion, ΔH^s is the heat of solid solution, and ΔS^f is the entropy of fusion of the impurity. By using the values of the heat of solid solution obtained from Eq. (3), the phase diagrams of the $NaNO_3$–KNO_3, –$RbNO_3$ and –$CsNO_3$ systems at very low impurity concentrations were constructed as shown in Fig. 3. The thermodynamic constants used in the calculations are listed in Table 3. The phase diagrams of other systems can be easily constructed by using the figures in Table 3. The solid solubilities of most of the impurities decreased as the temperature increased. However, a slight retrograde solid solubility is observed for the system containing $CsNO_3$ between 450 and 500 K. It is rather interesting that a retrograde solid solubility is found in an ionic crystal system such as this one.

REFERENCES

1. Y. Ikeda, *Denshi Zairyo (Electronics Materials), 13*(8), 40 (1974).
2. A. D. Peason, Xth Int. Congr. Glass, *6*, 31 (1974).
3. W. G. Pfann, *Zone Melting*, Wiley, New York, 1966.
4. Y. Hoshino, T. Utsunomiya, and K. Fukui, *Nippon Kagaku Kaishi*, No. 11, 1672 (1976).
5. Chemical Society of Japan, *Jikken Kagaku Koza, Suppl. 2*, Maruzen, 1967, p. 522.
6. J. A. Burton, R. C. Prim, and W. P. Slichter, *J. Chem. Phys., 21*, 1987 (1953).
7. Y. Hoshino and T. Utsunomiya, *J. Chem. Eng. Data, 27*, 144 (1982).
8. T. Utsunomiya and Y. Hoshino, *Report RLEMTIT, No. 7*, 1982, 37 p.
9. For example, N. K. Voskresenskaya, *Handbook of Solid–Liquid Equilibria in Systems of Anhydrous Inorganic Salts*, Israel Program for Scientific Translation Ltd.: E. M. Levin,

C. R. Robbins, and H. F. McMurdie, *Phase Diagrams for Ceramists,* American Ceramic Society, 1964.
10. D. J. Rogers and G. J. Janz, *J. Chem. Eng. Data, 27*(4), 424 (1982).
11. D. H. Hissink, *Z. Phys.* Chem., *32*, 545 (1900).
12. V. A. Palkin, *Zh. Obshch. Khim., 19,* 411 (1949).
13. R. A. Swalin, *Thermodynamics of Solids,* Wiley, New York, 1962.
14. C. D. Thurmond and J. D. Struthers, *J. Phys. Chem., 57,* 831 (1953).
15. K. Weiser, *J. Phys. Chem. Solids, 7,* 118 (1958).
16. For example, I. Barin and O. Knacke, *Thermochemical Properties of Inorganic Substances,* Springer, Berlin, 1973.
17. T. B. Douglas, *J. Chem. Phys., 45*(12), 4571 (1966).
18. C. Neogy and S. K. Deb, *J. Phys. Chem. Solids, 41,* 1381 (1980).
19. G. R. Allakhverdov and M. Yu. Zablotskaya, *Russ. J. Phys. Chem., 54*(2), 290 (1980).
20. V. S. Ursov, *Ibid., 43*(12), 1703 (1969).

Received by editor November 22, 1983